JOURNAL OF MATERIALS SCIENCE 28 (1993) 2664–2668

# Microstructure and properties of a Fe–C–Cu–$MoS_2$ alloy prepared by laser sintering

HU JIANDONG, LI YULONG, LI ZHANG
*Microanalysis Centre, Jilin University of Technology, Changchun, 130025 People's Republic of China*

BU XIANZHANG
*Changchun Institute of Optics and Fine Mechanics, Changchun, People's Republic of China*

WANG LICHUN
*Changchun Powder Metallurgy Factory, Changchun, People's Republic of China*

A laser beam was used to sinter green compacts of alloy powder. Elemental diffusion occurred during laser sintering, forming refined $Fe_3C$ and $CuMo_2S_{5-x}$ phases. Laser sintering can produce useful parts of desirable microstructure and good properties which offers advantages over those parts prepared by conventional sintering. A green compact with a diameter of 10 mm can be penetratively sintered within 5 min, showing the prospect for industrial applications.

## 1. Introduction

A laser with high power density is usually used for surface alloying and hardening of some metals. In the present study, a laser beam was employed to sinter the green compacts of alloy powder, giving the possibility of introducing laser sintering into the field of powder metallurgy. The method used in this work is thus named laser sintering of alloy powder (LSAP). Laser surface alloying is known as a powerful tool for modifying surface properties of metals and has found various applications. Laser alloying utilizes a high-power laser to melt alloy powders that are predeposited on the metal substrate. Only a very thin alloy layer can be achieved by this method (usually less than 1 mm). LSAP is, on the other hand, a material-fabrication method which uses a laser beam to sinter the green compact consisting of alloy powders, thus producing various alloy materials. It offers the following advantages: (i) energy saving; (ii) limitation of the deformation of parts, and (iii) microstructure refining. Although there is a size limit for the green compact, LSAP as a new sintering method can be used in some areas, as shown in our earlier work [1]. The purpose of the present study was to investigate microstructure and properties of the laser-sintered compacts, and to try to promote further interest in laser sintering.

## 2. Experimental procedure

The composition of the alloy (wt %) used was 1.6C, 2.5Cu, and 2.5$MoS_2$ (iron balance). The particle size of the first three powders was all 200 mesh, while the iron particles were 80–100 mesh. The powder mixture was extruded into specimens using a hydraulic press at a pressure of $4.6 \times 10^8 N/m^2$. The specimen was 10 mm in diameter. A 2 kW $CO_2$ laser generator was used to sinter the specimens with a sintering time of 5 min for each specimen, and the laser beam was focused to 40 mm diameter. Some specimens were coated with active carbon before laser sintering. Microhardness was measured for each specimen after sintering on a tester using a load of 100 g.

A sample-on-wheel reciprocating wear-test machine was used. The samples were clamped to the wear machine. A friction wheel made of an alloy with a hardness of 75HRc was employed to wear the sintered materials. The friction wheel was run at a speed of 200 r.p.m. with an applied load of 20 kg; wear time was 30 min for each sample. A balance with an accuracy of 0.1 mg was used to determine the weight loss of the worn samples.

The cross-sections of the tensile specimens were all 6 mm × 6 mm with a gauge length of 40 mm. The size of the impact specimen was 10 mm × 10 mm (cross-section) × 55 mm without any notch. The pressed specimens were then sintered by laser using the parameters mentioned above. The tensile test was carried out on an Instron machine and dynamic instrumented impact tests were used to evaluate the impact fracture toughness. The morphology of the samples was observed with an SEM. X-ray diffraction was carried out on a D/max-rA type diffractometer employing a $CuK_\alpha$ radiation and a graphite filter.

## 3. Results and discussion

### 3.1. Porosity

Fig. 1 shows the morphology of the laser-sintered materials. The average volume fraction of porosity measured was 12 %.



0022–2461 

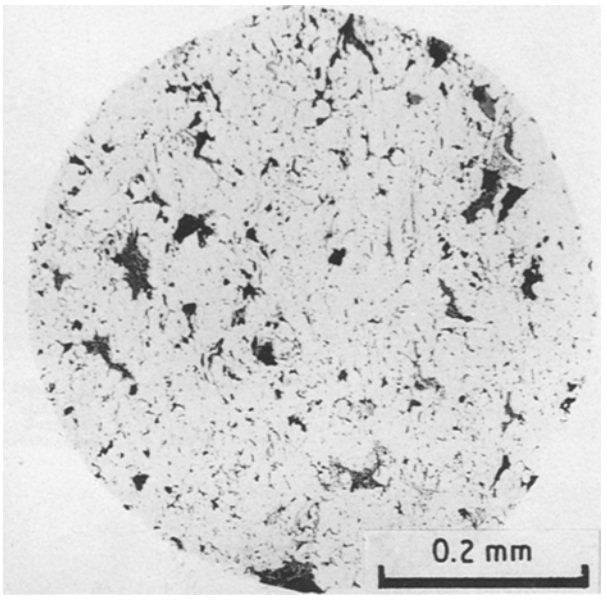


*Figure 1* Optical micrograph, showing porosity of the laser-sintered specimen, unetched.

## 3.2. Microhardness

Microhardness was tested along the whole cross-section of the laser-sintered specimens. Its values are shown in Table I. Data for the conventional sintering in Table I were obtained from specimens sintered in a furnace at 1050 °C for 2 h, and all values are the average of three measurements. As can be seen, higher hardness value is achieved and the whole cross-section of the green compact has been sintered by laser.

## 3.3. Wear resistance

Table II shows results from the wear tests for both laser and conventionally sintered materials. Through the wear test, we notice that the laser-sintered specimens have almost the same weight loss as those conventionally sintered.

Fig. 2a and b show the worn surface of a laser-sintered specimen. Many fine, smooth and uninterrupted "plough ditches" are observed. We also found some abrasive areas which resulted from adhesion during the wear test. Thus, it is believed that abrasion is the main wear mechanism for the laser-sintered specimens. Compared with the laser-sintered material, the worn surfaces of those conventionally sintered have relatively more and larger adhesive areas as shown in Fig. 2c and d. Accordingly, adhesion plays an important role in this material during the wear test. Generally, for the materials with a relatively low hardness, adhesion will be dominant during sliding wear. It is concluded through SEM observations that the laser-sintered material possesses better resistance to wear, which can be related to its high hardness level.

## 3.4. Properties

Sintering parameters of Group 1 are the same as Group 2; Groups 3 and 4 are the same as shown in Table III. There is no clear correlation for the yield strength, $Y_s$, values of the specimens with and without the active carbon coating. It is, however, noted that the specimens coated with active carbon possess much better $\delta$ and $a_k$ values than those without coating. This indicates that oxidization occurred during laser sintering and that it can be prevented by carbon coating. As shown in Table III, the specimens coated with active carbon have good composite mechanical properties (all values shown in Table III are averaged values obtained from three specimens and no stress–strain curves are recorded).

## 3.5. Microstructure

Fig. 3a shows lamellar pearlite and net cementite for the laser-sintered specimens. The lamellar pearlite exists in the form of a colony and the net cementite predominantly precipitates at grain boundaries. It is interesting to note that some spheroidal cementite is distributed in the ferrite, as shown in Fig. 3b. The average size of the spheroidal cementite is below 2 μm.

Most of the laser power can be reflected when metals are irradiated by a laser beam. For example, 90–98% of the incident laser power will be reflected away from most polished metal surfaces when its power density is less than $10^5$ W/cm$^{-2}$ [2]. In the case where the green compacts are irradiated, the absorptivity of the irradiated surfaces will increase because there is a relatively high porosity (12%) on the

TABLE I Microhardness distribution along the cross-section of the laser-sintered specimen

| Distance from the surface (mm) | Microhardness (100 g) Hv | |
|---|---|---|
| | Laser sintering | Conventional sintering |
| 2 | 130 | 125 |
| 4 | 150 | 120 |
| 6 | 142 | 115 |
| 8 | 125 | 132 |

TABLE II Values of weight loss

| | Weight before wear (g) | Weight after wear (g) | Weight loss (g) |
|---|---|---|---|
| Laser sintering | 3.4958 | 3.4825 | 0.0133 |
| Conventional sintering | 4.3146 | 4.3021 | 0.0125 |

TABLE III Properties of laser-sintered specimens

| | $Y_s$ (GPa) | $\delta$(%) | $a_k$(J/cm$^2$) | Carbon coated |
|---|---|---|---|---|
| 1 | 0.020 524 | 4.811 30 | 5.184 | Yes |
| 2 | 0.964 7 | 2.004 00 | 3.175 | Yes |
| 3 | 0.066 649 | 0.998 00 | 2.422 | No |
| 4 | 0.043 61 | 0.598 00 | 2.852 | No |

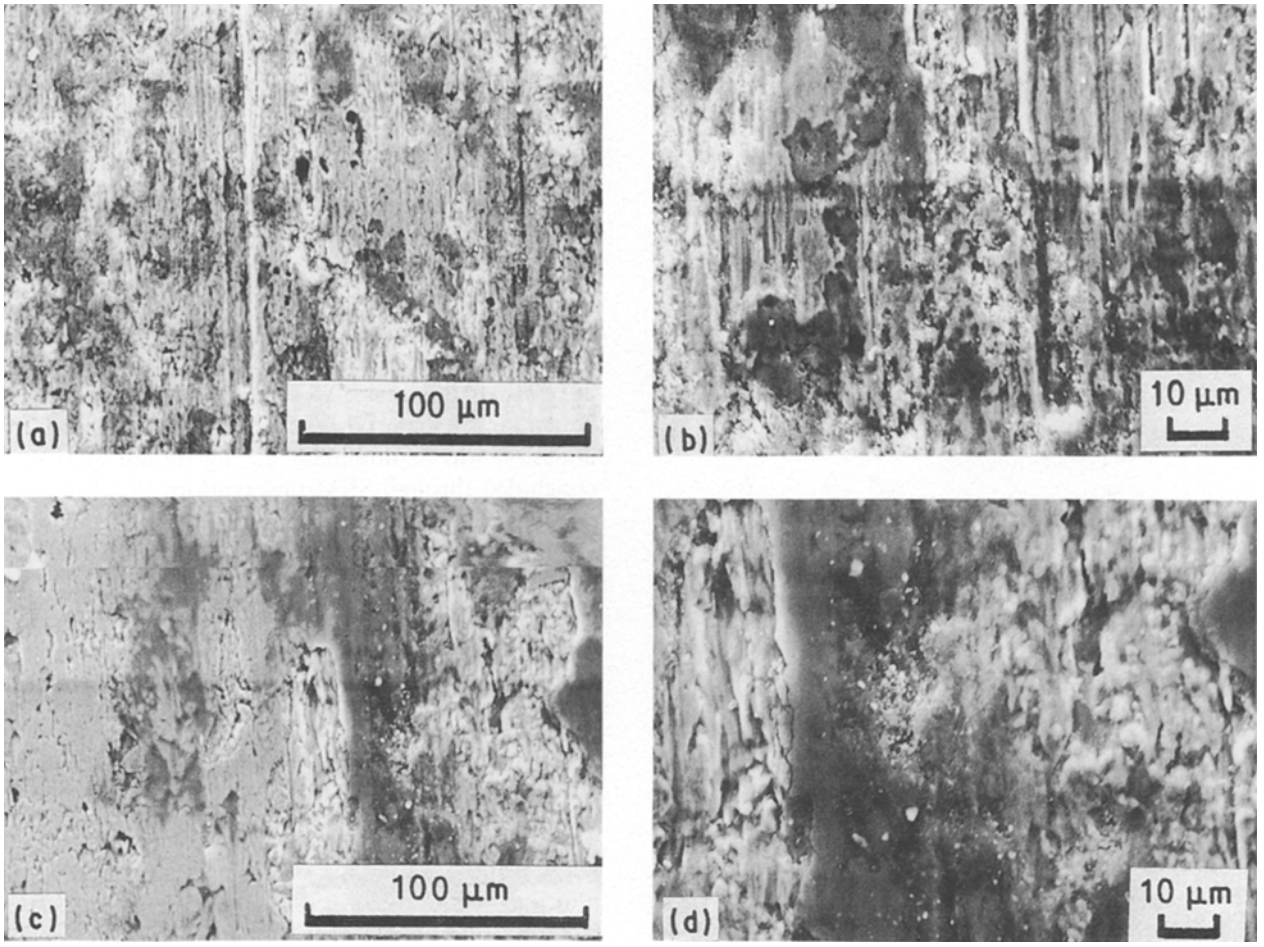


*Figure 2* A series of scanning electron micrographs showing worn surfaces of (a, b) a laser-sintered specimen, (c, d) conventionally sintered specimen.

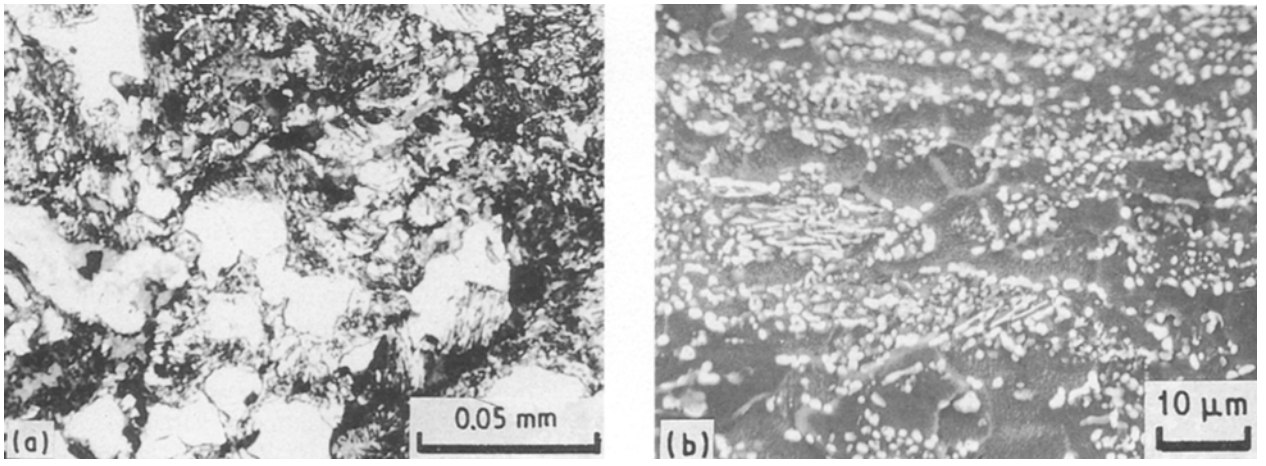


*Figure 3* Micrographs showing the microstructure of the laser-sintered specimen: (a) an optical micrograph showing pearlite colony, (b) a scanning electron micrograph showing spheroidal cementite.

surface. Therefore, it is easy for the green compact to be heated to the critical phase temperature at which austenite is formed resulting from the carbon diffusion from graphite to iron. In Gregson's paper [2], a pearlite grain was taken as an example to describe the formation of austenite resulting from the carbon carbide ($Fe_3C_3$) to ferrite and the decomposition of the formed austenite when it is heated by laser and cooled by conducting heat through itself. In our case, austenite is formed, but the cooling rate is much slower. This cooling rate allows the austenite to reform pearlite by the carbon diffusing into iron grains.

In addition to $Fe_3C$, $CuMo_2S_{5-x}$ phases were also detected by X-ray diffractometry (XRD). The XRD pattern is shown in Fig. 4. SEM observations also revealed some phases which are rich in both copper and molybdenum as confirmed by D. Fig. 5a–c show micrographs of the typical morphology and the ele-

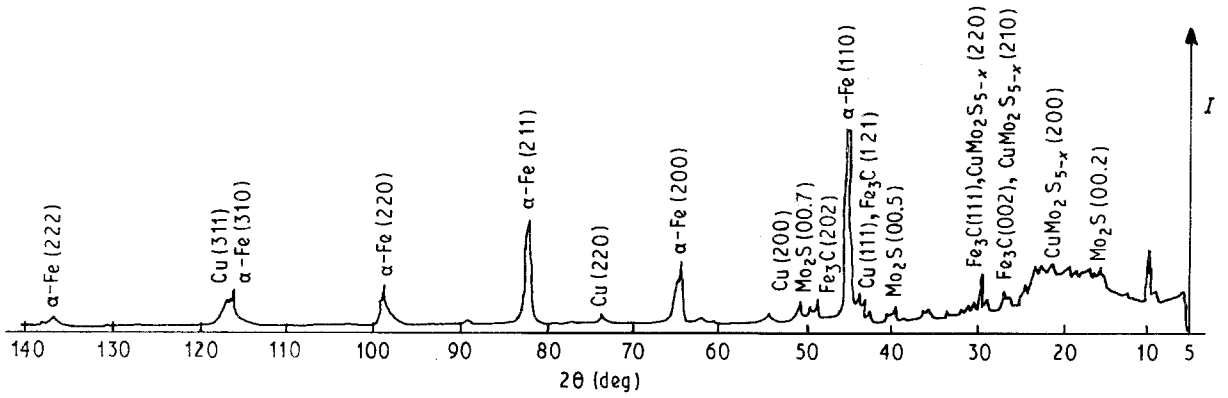


*Figure 4* X-ray diffraction pattern.

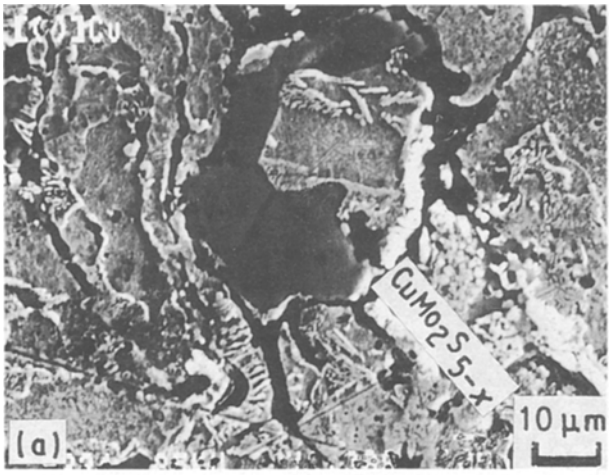


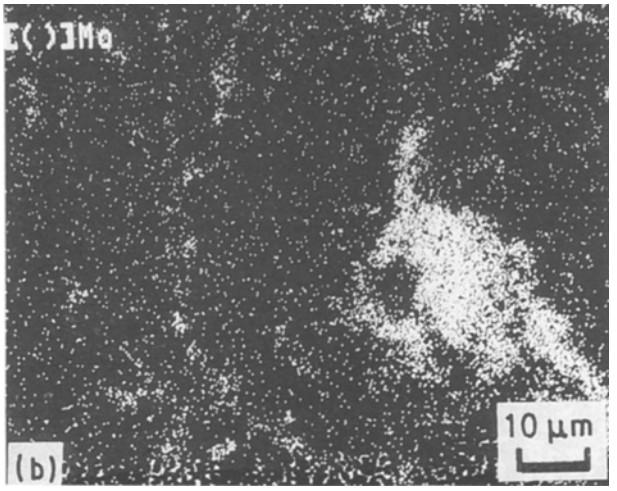


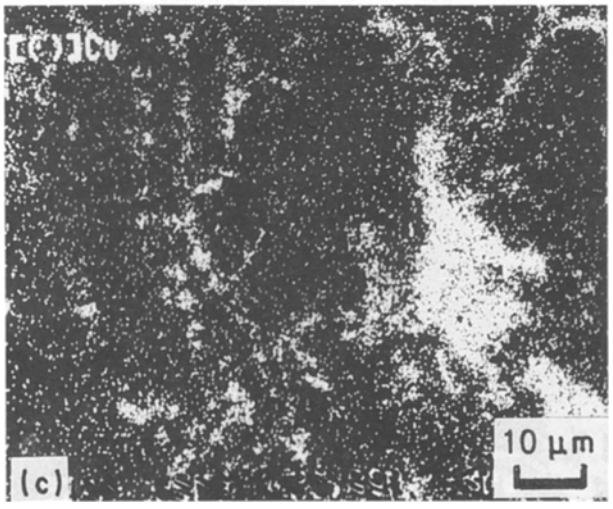


*Figure 5* A series of scanning electron micrographs: (a) morphology of the phase rich in molybdenum and copper, (b) molybdenum distribution, (c) copper distribution.

mental distribution for the phase rich in copper and molybdenum, which may exist in the form of $CuMo_2S_{5-x}$.

The green compact contains a number of grains of copper and $MoS_2$. It is believed that the formation of the $CuMo_2S_{5-x}$ phase results from the copper diffusion from the copper grain into $MoS_2$ grains. For the alloy powder sintering, three diffusion mechanisms (volume, surface and grain-boundary diffusions) were reported in Johnson's early studies (3). These three mechanisms may all work in the present case. However, a special effect must also be taken into account in the case of laser sintering. For example, specimens are generally subjected to a pressure caused by the laser-beam irradiation. The value of pressure reported by Draper and Poate [4] was up to the order of 10 GPa when the energy density was in the range 22–35 J $cm^{-2}$ with a pulse length of 25 ns. This can induce an increase in surface contact area between the alloy powders and thereby affect element diffusion. A number of publications [5–7] have manifested that diffusibility could be enhanced by the external pressure. This in turn can be employed to explain why laser sintering can produce good alloy powder products.

## 4. Conclusion

Cu, C, $MoS_2$ and Fe diffusion occurred during laser sintering, resulting in the formation of $Fe_3C$ and $CuMo_2S_{5-x}$. Specimens with a diameter of 10 mm can be fully sintered within 5 min. The values of the microhardness across the whole cross-section of the specimen remain relatively unchanged and the desirable toughness and strength are achieved when using preventative coating. This work shows the possibility of using LSPA in industrial applications.

## References


1. HU JIANDONG and LI ZHANG, "Laser Sintering of Some Alloy Powder Parts", Chinese Pat. 9011 010 414, 20 December 1990.
2. V. G. GREGSON, in "Laser Heat-Treatment in Laser Materials Processing", "Materials Processing Theory and Practices", Vol. 3, edited by M. Bass (North-Holland, 1983) pp. 206–19.
3. D. L. JOHNSON, *J. Appl. Phys.* **40** (1969) 192.
4. C. W. DRAPER and J. M. POATE, *Int. Met. Rev.* **30** (1985) 85.
5. P. G. SHWMON, "Diffusion in Solids", (McGraw-Hill, 1963) pp. 281.
6. L. A. GIRIFALCO, in "Metallurgy at High Pressures and Temperature", edited by K. A. Gachneider, M. T. Hepworth, and N. A. D. Parlee (Gordon and Breach, 1964) pp. 260.
7. D. SUBRAMANYAM, M. R. NOTIS and J. I. GOLDSTEIN, *Metall. Trans.* **16A**(4) (1985) 605.



*Received 23 September 1991*
*and accepted 30 October 1992*